Fuel 182 (2016) 141–153

Contents lists available at ScienceDirect

Fuel

journal homepage: www.elsevier.com/locate/fuel

Full Length Article

Reliable characterization of bitumen based on perturbation from n-alkanes for steam-solvent coinjection simulation

Ashutosh Kumar [a], Ryosuke Okuno [b,*]

[a] University of Alberta, Canada
[b] University of Texas at Austin, USA

HIGHLIGHTS

- Six bitumens are characterized by the perturbation from n-alkanes (PnA) method.
- With the PnA method, gas solubilities in bitumens are successfully modeled.
- The effect of fluid characterization on flow simulation is analytically evaluated.

ARTICLE INFO

Article history:
Received 9 January 2016
Received in revised form 17 May 2016
Accepted 20 May 2016
Available online 26 May 2016

Keywords:
Bitumen
Fluid characterization
Equation of state
Perturbation from n-alkanes
Steam-assisted gravity drainage
Steam-solvent coinjection

ABSTRACT

Bitumen recovery by steam-solvent coinjection involves the coupled thermal/compositional mechanisms for reduction of bitumen viscosity. Reliable design of such processes requires reservoir flow simulation based on a proper phase-behavior model so that the oleic-phase viscosity near the steam-chamber edge can be modeled reliably. However, the effect of bitumen characterization (e.g., the number of pseudo components used) on steam-solvent coinjection simulation has not been studied in detail, and can be realized only after running multiple reservoir simulations, which is time consuming.

There are two main objectives in this paper. One is to develop a reliable method for bitumen characterization by improving the fluid characterization method that was recently developed based on perturbation from n-alkanes (PnA). The other is to develop a novel analytical method for assessing the sensitivity of a particular coinjection simulation to bitumen characterization without having to perform reservoir simulations. A simulation case study is given to validate this analytical method.

A proper number of pseudo components for bitumen characterization cannot be determined without considering the effect of phase behavior on the oleic-phase viscosity at chamber-edge conditions in steam-solvent coinjection simulation. Results show that the analytical method developed in this research can detect the sensitivity of recovery simulation to bitumen characterization without performing multiple flow simulations using different sets of fluid models. The PnA-based method developed for bitumen characterization gives reliable predictions of phase behavior for bitumen/solvent mixtures with a small amount of experimental data.

1. Introduction

Steam-assisted gravity drainage (SAGD) is a widely-used method for in-situ bitumen recovery [1,2]. The most important mechanism in SAGD is the reduction of the oleic-phase (L-phase) viscosity owing to the heat that the injected steam releases when condensing into hot water near the steam-chamber edge. The main drawback of SAGD is the substantial usage of steam, which may also cause various environmental concerns.

Coinjection of solvent with steam, such as expanding-solvent steam-assisted gravity drainage (ES-SAGD), has been proposed and pilot-tested to improve the efficiency of SAGD [3,4]. In ES-SAGD, a small amount of hydrocarbon solvent (e.g., a few percent by mole) is coinjected with steam. It aims to reduce the L-phase viscosity by diluting bitumen with condensed solvent, in addition to the thermal mechanism, along the chamber edge.

Unlike SAGD, ES-SAGD involves multiphase behavior of solvent/bitumen mixtures at a wide range of temperature and its interaction with non-isothermal flow under heterogeneities. The

* Corresponding author at: Department of Petroleum and Geosystems Engineering, University of Texas at Austin, 200 E. Dean Keeton Street, Stop C0300, Austin, TX 78712, USA.
E-mail address: okuno@utexas.edu (R. Okuno).

http://dx.doi.org/10.1016/j.fuel.2016.05.095
0016-2361/

Nomenclature

AARD	average absolute relative deviation $= \frac{1}{M}\sum_{j=1}^{M}\left\lvert\frac{\text{prediction-data}}{\text{Data}}\right\rvert_j$
AAD	average absolute deviation $= \frac{1}{M}\sum_{j=1}^{M}\lvert\text{prediction-data}\rvert_j$
BIP	binary interaction parameter
CN	carbon number
ES-SAGD	expanding-solvent steam-assisted gravity drainage
L–L	liquid (L)–liquid (L) phase equilibrium
L–V	liquid (L)–vapor (V) phase equilibrium
N_C	number of components
PC	pseudo components
PR EOS	Peng and Robinson [18,19] equation of state
SAGD	steam-assisted gravity drainage
T–x	temperature–composition

Greek symbols

δ	deviation of calculated saturation pressure from experimental value
δ_{TOL}	tolerance for deviation δ
ε	AARD for density prediction
ε_{TOL}	tolerance for deviation ε
μ	viscosity
μ_{edge}	viscosity of the L phase in equilibrium with the other two phases at a chamber edge
ρ_L	molar density of the liquid phase (Eq. (12))
ρ_{iL}	effective molar density of the ith component in the liquid phase (Eq. (12))
γ	specific gravity
ψ	parameter defined in Eq. (1).
x_{SL}	solvent mole-fraction in the oleic phase in equilibrium with the other two phases.
ω	acentric factor

Symbols

a	attraction parameter in a cubic equation of state
b	covolume parameter in a cubic equation of state
f_b	perturbation parameter for covolume
f_ψ	perturbation parameter for ψ as shown in Eqs. (3) and (4)
D_N	experimental density data
D_{N_EOS}	predicted density
k_{sb}	binary interaction parameter for the solvent-bitumen pair (Eq. (11))
MW	molecular weight
n	number of pseudo components
m	parameter in the PR EOS as a function of acentric factor
m_b	parameter defined in Eq. (2).
P_C	critical pressure
PC	pseudo components
P_S	experimental saturation pressure
P_{S_EOS}	calculated saturation pressure with the PR EOS
T_b	boiling-point temperature
T_C	critical temperature
T_e	chamber edge three-phase temperature
$V_{C,b}$	critical volume of bitumen
$V_{C,S}$	critical volume of solvent

Subscript

i	index for pseudo component
mix	mixture
s	solvent
L	liquid hydrocarbon phase
w	water
W	liquid water phase
V	vapor phase

Superscript

Vap	vapor pressure

efficiency of ES-SAGD is substantially dependent on pressure, temperature, and composition near the chamber edge, in which the condensation of steam and solvent and the mixing of solvent with bitumen take place through gravity drainage [5].

Due to the complexity, design of ES-SAGD requires numerical simulation that accommodates the compositional effect on non-isothermal reservoir flow. Numerical simulation studies have been presented in the literature to understand various aspects of this complex process [3,6–8]. However, the effect of fluid characterization on ES-SAGD simulation has not been investigated in detail, although such simulations are directly affected by how the fluid is characterized.

Fluid characterization for ES-SAGD simulation is challenging because it requires a reliable method for modeling phase properties that does not give physically absurd values at a wide range of composition and temperature for the operating range of pressure. For example, the temperature range in ES-SAGD can be from 300 K to 500 K. The L-phase composition can vary widely from nearly 100% solvent to 100% bitumen in the vicinity of the chamber edge.

Several researchers used conventional characterization methods to develop equation-of-state (EOS) models to represent bitumens and their gas solubilities [9–12]. The conventional methods have three main steps: (1) representation of bitumen by a user-defined number of pseudo components, (2) estimation of pseudo components' parameters, such as critical temperature (T_C), critical pressure (P_C), acentric factor (ω), and critical volume (V_C), using various correlations, and (3) regression of the parameters to match experimental data.

Step 1 of the conventional method uses atmospheric and vacuum distillation data. Bitumens are represented by SARA (saturate, aromatic, resin, and asphaltene) fractions or by pseudo components obtained from a certain probability distribution function, such as the gamma distribution function [13]. Step 2 of the conventional method estimates T_C. P_C, and ω for pseudo components using correlations that are functions of normal boiling point (T_b) and specific gravity (γ). Binary interaction parameters (BIPs) are also estimated as functions of one or more parameters, such as T_C, P_C, V_C, and ω. In Step 3 of the conventional method, T_C, P_C, ω, and BIPs of pseudo components (estimated in Step 2) are adjusted to match compositional phase-behavior data of bitumen such as gas solubilities. Then, density (or volumetric) data are matched by adjusting only volume shift parameters. The objective of Step 3 is to reduce the deviation of EOS predictions from experimental phase behavior data because the general correlations used in Step 2 tend to be in substantial error when extrapolated to high carbon numbers (CNs) relevant to bitumen components.

The number of pseudo components used for bitumen characterization substantially affect the computational efficiency of bitumen-recovery simulation [14]. The number of pseudo components required for the conventional method to match experimental data ranges up to 6 in the literature [10–12,15,16]. Attempts to represent bitumen by a single pseudo component have not been successful [10,11]. This may be due to uncertainties in conven-

tional bitumen characterization from multiple sets correlations with unknown reliabilities in Step 2, many adjustable parameters used in Step 3, and a high level of uncertainties in bitumen data. It is unknown in the literature whether characterization of bitumen/solvent mixtures, although challenging, requires as many as 6 pseudo components for thermal flow simulation. Use of more pseudo components certainly offers the flexibility in matching experimental data; however, the correlative accuracy obtained with a large number of pseudo components does not necessarily yield accurate predictions of phase behavior during thermal flow simulation due to a wide range of thermodynamic conditions encountered.

Various issues of conventional characterization methods were discussed by Kumar and Okuno [17]. They used the method of perturbation from n-alkanes (PnA) to characterize various reservoir fluids, except for bitumens, by direct perturbation of attraction (a) and covolume (b) parameters. It was shown that the reservoir fluids studied were characterized reliably by adjusting a and b parameters to match compositional and volumetric data. Volumetric data were effectively used to capture the level of aromaticity of the fluid of interest in the PnA method, which is not the case with conventional methods using volume shift. Use of volumetric data for determination of the a and b parameters is particularly important for characterization of bitumens, because they are highly aromatic. However, the PnA method for bitumen characterization was not studied in Kumar and Okuno [17], and will be presented in this research for the first time.

Even with a reliable method, it is important to ensure that the simulation results are not sensitive to the phase-behavior model used. This is because fluid characterization for ES-SAGD is performed under inherent uncertainties in terms of experimental data. It would not be easy to measure phase properties at the thermodynamic conditions that occur during ES-SAGD, even if such conditions could be precisely predicted. Different fluid models created under such uncertainties may give a similar level of correlative accuracy for the limited experimental data available; however, they do not necessarily give similar results in numerical reservoir simulation, in which phase behavior should be predicted at a variety of thermodynamic conditions. Currently, there is no method for assessing the sensitivity of simulation results to the phase-behavior model without performing actual flow simulations. As will be shown in this paper, a proper number of pseudo components in bitumen characterization cannot be determined without consideration of compositional effects on the oil recovery process of interest, which is ES-SAGD in this paper.

There are two main objectives in this research. The first objective is to show reliable characterization of bitumen by using the improved method that was developed by the authors (Section 2). It is also shown that the proposed method of bitumen characterization can decrease the number of pseudo components required to match gas solubilities in bitumens to one, without significantly affecting phase-behavior predictions. The second objective is to develop a novel method for analytically assessing the sensitivity of ES-SAGD simulation to the phase behavior model used (Section 3). The analytical method is validated in the simulation case study (Section 4).

2. Bitumen characterization based on perturbation from n-alkanes

This section presents characterization of six different bitumen samples using the Peng–Robinson equation of state (PR EOS) [18,19] along with the van der Waals mixing rules on the basis of perturbation from n-alkanes (PnA). Direct perturbation of the a and b parameters by the PnA method [17] is applied to bitumens for the first time. The main difference between the PnA method and the conventional method of bitumen characterization lies in how pseudo components' properties are adjusted during the regression of an EOS model to phase-behavior data.

The PnA method for bitumen characterization is presented in Section 2.1, and applied to actual bitumen/solvent mixtures in Section 2.2. Section 2.3 describes the significance of the PnA method to obtain reliable trends of EOS-related parameters for pseudo components.

2.1. Algorithm for bitumen characterization by direct perturbation from n-alkanes

The PnA method begins with a PR-EOS model calibrated for n-alkanes; hence, pseudo components are initially assumed to be n-alkanes. Then, the a and b parameters for pseudo components are adjusted in the direction of increasing aromaticity from n-alkanes (i.e., zero aromaticity) until a saturation pressure and densities at a given temperature are matched for the fluid of interest. Volumetric and compositional phase behavior are corrected largely by adjusting the b parameter to match densities and by adjusting the ψ parameter to match a saturation pressure, respectively. As shown in the original PnA method [17], the ψ parameter is

$$\psi = a/b^2, \quad \text{or} \quad \frac{\Omega_a}{\Omega_b^2} P_C \left(1 + m\left[1 - (T/T_C)^{0.5}\right]\right)^2 \tag{1}$$

on the basis of the PR EOS. Parameter "m" is a function of ω, and Ω_a and Ω_b are the constants for the attraction and covolume parameters as defined by Peng and Robinson [18,19].

The two types of experimental data, density and saturation pressure, are important in the PnA method since the b and ψ parameters are adjusted specifically for volumetric and compositional predictions, respectively. In this research, such experimental data are taken from a bitumen/gas mixture, because a bitumen sample often exhibits no obvious saturation pressure even at 450 K, which is near the highest operating temperature of the conventional phase-behavior experimental setup. More specifically to this paper, we use the saturation pressure and density data for the bitumen saturated with methane around 373.15 K (100 °C), although the selection of gas and temperature is arbitrary in principle. The BIPs of methane with bitumen components are set to zero in this paper, although other default values are also possible.

As presented in [17], the adjustment of the b parameter for matching density data is performed through the following equation:

$$b_i = -14.6992113939827 + 1.36977232166027\left(\frac{MW_i}{m_{bi}}\right) - 9.12089276536298 \times 10^{-5}\left(\frac{MW_i}{m_{bi}}\right)^2, \tag{2}$$

where i is the index for pseudo components, $m_{bi} = (MW_i/86.0)^{f_b}$, and MW_i is the molecular weight of component i. The f_b perturbation parameter is zero for n-alkanes, and increases with increasing level of aromaticity in terms of volumetric phase behavior. The m_{bi} parameter increases with MW for a given f_b value.

The a parameter is adjusted through the ψ parameter for a given b parameter (i.e., $a = \psi b^2$). Kumar and Okuno [17] observed that reasonably accurate predictions of phase behavior at a given temperature could be obtained by using a linear relationship between ψ and MW for pseudo components. Such a linear relationship is referred to as "linear ψ" in this paper. They also observed that the slope of linear ψ with respect to MW is nearly constant for pseudo components heavier than C_{20} (as is the case with bitumen components), and that the y-intercept of linear ψ with respect to MW increases with increasing level of aromaticity. In this

research, therefore, ψ's of pseudo components are perturbed using the following linear function ψ with respect to MW:

$$\psi_i = -0.9415\mathrm{MW}_i + 2495.8 f_\psi. \quad (3)$$

Eq. (3) represents the reference ψ line corresponding to n-alkane values when the f_ψ perturbation parameter is the initial value of 1.0. This reference ψ line is based on the optimized a and b parameters for the PR EOS to give accurate phase behavior predictions [17,20]. The coefficients in Eq. (3) are temperature-specific (373.15 K in this case) because of the temperature dependency of the a parameter in the PR EOS. The ψ function can be systematically increased by increasing the f_ψ perturbation parameter from the initial value of 1.0, which increases the y-intercept of the function.

When only one pseudo component is used, the ψ parameter is adjusted by changing the f_ψ perturbation parameter in

$$\psi = \Psi_n f_\psi = (-0.9415\mathrm{MW} + 2495.8) f_\psi \quad (4)$$

where ψ_n is the ψ parameter calculated for an n-alkane with MW at 373.15 K. Again, the temperature selection is arbitrary as long as it is relevant to the application of interest and consistent among Eqs. (3), (4), and experimental data. In this paper, 373.15 K was selected considering available data.

Unlike the conventional method, the PnA method systematically changes the vapor pressure curves of all pseudo components through direct adjustment of the two parameters. Fig. 1 shows the change in phase envelope for an example mixture of bitumen and methane, in which bitumen is represented by a single pseudo component. The solid curve in this figure is the initial phase envelope for which the bitumen is assumed to be an n-alkane (i.e., $f_b = 0.0$ and $f_\psi = 1.0$). The other curves correspond to positive levels of aromaticity of the bitumen (i.e., $f_b > 0.0$ and $f_\psi > 1.0$). A step-wise description of the algorithm is given below. A flow chart is also presented in Appendix A to further describe the algorithm.

Step 1. Compositional characterization

This step is required only when bitumen is to be represented by multiple pseudo components. The chi-squared distribution function [21] is applied to split bitumen into pseudo components. Quiñones-Cisneros et al. [21] observed in their study that the degree of freedom of 10 was sufficient for the heavy oils tested. In this work, the degree of freedom of 12 is assumed for bitumen. The C_{7+} molecular weight is taken from the molar mass reported for the bitumen sample of interest. The bitumen is split into a desired number (n) of pseudo components with equal mass fractions. Lolley and Richardson [14] recommended use of at least four pseudo components for reliable thermal recovery simulation. Accordingly, four pseudo components (i.e. $n = 4$) are used for multicomponent representation of bitumen, although single-component representation by use of the PnA method is presented in this paper. Set $f_b = 0.0$, and $f_\psi = 1.0$.

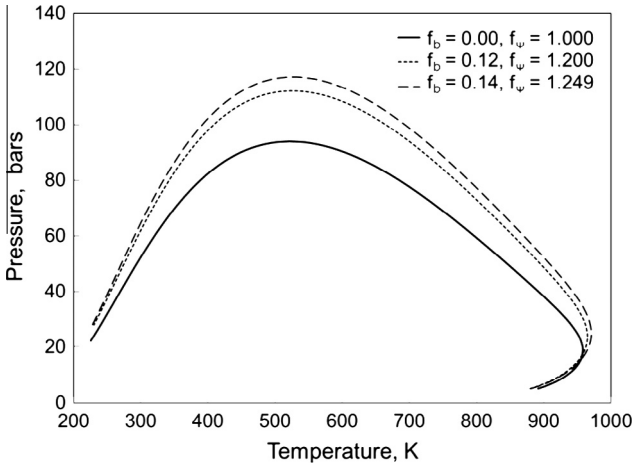

Fig. 1. Systematic development of phase envelope for a sample mixture of bitumen and methane during the regression using the algorithm developed in this research. The phase envelope expands with increasing f_b and f_Ψ.

Step 2. Initialization of the a and b parameters for each pseudo component

Eq. (2) is used for covolumes, b_i, for $i = 1, \ldots, n$. Eq. (3) is used for ψ_i ($i = 1, \ldots, n$) if $n > 1$. Otherwise, Eq. (4) is used. Then, the a parameter is calculated by $a_i = \psi_i b_i^2$ for each pseudo component.

Step 3. Perturbation of f_ψ to match the saturation pressure

Calculate $\delta = (P_S - P_{S\_EOS})/P_S$, where P_S is the saturation pressure measured for a bitumen/methane mixture at 373.15 K as discussed previously. P_{S_EOS} is the calculated saturation pressure, and δ is the average absolute relative deviation (AARD) in saturation pressure. If $\delta < \delta_{TOL}$ (e.g., 10^{-4}), go to Step 4. Otherwise, increase f_ψ (i.e. $f_\psi = f_\psi + \Delta f_\psi$; $\Delta f_\psi = 10^{-4}$) and go to Step 2.

Step 4. Perturbation of f_b to match the saturated liquid density

Calculate the AARD in density, ε, as $(D_N - D_{N\_EOS})/D_N$, where D_N is the density at the saturation point used in Step 3, and D_{N_EOS} is the calculated density. If $\varepsilon < \varepsilon_{TOL}$ (e.g., 10^{-3}), stop. Otherwise, increase f_b (i.e., $f_b = f_b + \Delta f_b$; $\Delta f_b = 10^{-4}$), reset f_ψ to 1.0, and go to Step 2.

Step 5. Conversion of the final set of the a and b parameters to T_C, P_C, and ω

This step uses the procedure of Kumar and Okuno [17], in which a physically reasonable set of T_C, P_C, and ω is back-calculated from the final set of the a and b parameters from the PnA method. This calculation also gives T_b and γ for each pseudo component as it uses the Lee and Kesler [22] and Kesler and Lee [23] correlations. The correlation of Riazi and Daubert [24] can be used along with the T_b and γ to calculate V_C for each pseudo component.

2.2. Case studies for bitumen characterization

The algorithm presented in the previous subsection is used to characterize six bitumens: Athabasca [25,26], Cold Lake [27], Peace River [28], Wabasca [29], JACOS [30,31] and Surmont [30,31]. For each bitumen, data are available for methane/bitumen mixtures so that the algorithm can use the density at the methane-saturation pressure near 373.15 K (100 °C) in Steps 3 and 4. As mentioned previously, the BIPs for methane with pseudo components are set to zero for all cases in this paper.

The systematic change in pseudo components' properties during the regression allows to conduct a comparative study of bitumen characterization in terms of the number of pseudo components used. Hence, each bitumen is characterized by using four pseudo components (the 4-PC case) and one pseudo component (the 1-PC case). Table 1 shows the data used for the characterization and the converged values for f_b and f_ψ for each bitumen. The densities of methane-saturated bitumens, D_N, at P_S are similar to each other; therefore, no correlation is obvious for D_N and f_b. However, it is relatively clear that f_ψ increases with P_S, which comes from the systematic change in phase envelope in the PnA method. That is, the two-phase envelope for a bitumen/methane

Table 1
Data used in characterization, and regressed f_b and f_ψ values for bitumens characterized. AARDs shown are for prediction of methane solubility at pressure and temperature points other than that used in characterization.

Bitumen	Data used in characterization				1-PC (PnA characterization)			4-PC (PnA characterization)			Conventional characterization
	MW (g/mol)	X_{CH4} (%)[a]	P_S (bars)	D_N at P_S (g/CC)	f_b	f_ψ	AARD (%)	f_b	f_ψ	AARD (%)	AARD [12] (%)
Athabasca	594.6	26.17	94.40	0.9510	0.1420	1.2494	11.05	0.1353	1.2196	9.24	7.95
Cold Lake	533.0	18.95	51.60	0.9384	0.1517	1.0046	5.72	0.1447	1.0329	7.22	3.74
Peace River	527.5	25.19	76.50	0.9660	0.1718	1.0637	11.08	0.1643	1.0797	11.75	10.14
Wabasca	446.6	28.33	93.50	0.9310	0.1688	1.0857	8.35	0.1651	1.1056	11.23	7.51
JACOS	530.0	27.00	81.00	0.9440	0.1573	1.0378	15.78	0.1502	1.0588	16.76	
Surmont	540.0	27.00	80.00	0.9410	0.1585	1.0228	7.58	0.1513	1.0473	7.33	

[a] Mole fraction of methane in methane saturated bitumen at 373.15 K and P_S shown. Temperature in case of Athabasca is 372.95 K.

mixture gradually expands in pressure–temperature space as the perturbation proceeds (see Fig. 1).

For each bitumen, additional data available for methane solubilities are used to test the predictive accuracy of the resulting EOS model. Table 1 summarized the AARDs for these additional data. The AARD in methane solubility predicted for 99 temperature–pressure points for six bitumens is 10.75% with the 4-PC case and 10.44% with the 1-PC case. The difference is insignificant between the 4-PC and 1-PC cases likely because the relative volatility of methane to each pseudo component is not much different due to the substantial asymmetricity between methane and bitumen.

As reported by Mehrotra and Svrcek [10], some of the data for methane solubility in Athabasca bitumen are unreliable. For example, Table 1 shows that the PnA method yields the AARD of 9.24% in the 4-PC case and 11.05% in the 1-PC case for methane solubilities for Athabasca bitumen. However, if four unreliable data are excluded from the evaluation, the AARD reduces to 5.77% in the 4-PC case and 5.86% in the 1-PC case. Mehrotra and Svrcek [10] showed their characterizations of Athabasca bitumen excluding the four unreliable data, which gave the AARD of 4.9% using five pseudo components. Kariznovi et al. [12] reported the AARD of 7.95% using six pseudo components for Athabasca bitumen, but it is not clear how many data points were considered in the AARD.

A bitumen sample usually does not contain gas components, such as N_2, CO_2, and hydrocarbon gases. This is why the density at a saturation pressure for a gas/bitumen mixture is required for the PnA method to capture the compositional and volumetric phase behavior of bitumen through the a and b parameters. Although the density at a methane-saturation pressure was matched with zero BIPs for methane with bitumen components in this section, matching solubilities of a gas in a bitumen generally requires adjustment of their BIPs because the gas is not a part of the characterized bitumen. Such adjustment of BIPs is presented here for matching gas solubilities: N_2, CO_2, and C_2 for Athabasca [25,26], Cold Lake [27], Pease River [28], and Wabasca [29], C_2 for JACOS [31], and C_2, C_3, and C_4 for Surmont [30,31] (note that results for methane solubilities were presented in Table 1).

Table 2 shows the optimized BIPs and AARDs for the solubility data for these gases. As in Table 1, Table 2 presents the results for the 4-PC and 1-PC cases. The AARDs in the two cases are similar to each other; that is, bitumen characterization by the PnA method is insensitive to the number of pseudo components used for the cases tested. For comparison purposes, the last column of Table 2 presents the AARDs reported by Kariznovi et al. [12] with their conventional characterization of bitumen by using the PR EOS with six pseudo components. The comparison shows that use of one pseudo component may be sufficient, at least, for correlating experimental data using the PR EOS. However, a proper number of pseudo components should be evaluated in the context of flow in a specific reservoir process, which is ES-SAGD in this research. This will be discussed in detail in Section 3.

The AARD for ethane solubilities at 107 pressure–temperature points for all bitumens is 7.38% in the 4-PC case and 7.25% for the 1-PC case. Mehrotra and Svrcek [11] reported that at least three data points for Wabasca bitumen were unreliable. When these unreliable points are excluded, the AARD for the ethane solubility in Wabasca bitumen is 3.96% for the 4-PC case, 4.06% for the 1-PC case with the PnA method, and 4.1% by Mehrotra and Svrcek [11] using 3 pseudo components. Kariznovi et al. [12] reported the AARD of 6.56% using 6 pseudo components for Wabasca bitumen, although the number of data points considered is not clear in their

Table 2
Summary of case studies results. The AARDs for solubility data match for optimized BIPs are presented and compared with conventional characterization methods.

Bitumen	Gas	1-PC (PnA characterization)		4-PC (PnA characterization)		Conventional characterization
		Optimized BIP	AARD (%)	Optimized BIP	AARD (%)	AARD [12] (%)
Athabasca [25,26]	N_2	0.078	11.51	0.079	11.50	10.57
	CO_2	0.088	5.60	0.088	5.60	9.34
	C_2H_6	0.012	4.78	0.013	4.82	5.52
Cold Lake [27]	N_2	0.175	6.00	0.175	5.94	5.62
	CO_2	0.096	4.34	0.096	4.30	8.89
	C_2H_6	0.031	7.50	0.032	7.35	7.64
Peace River [28]	N_2	0.068	11.78	0.068	11.79	14.40
	CO_2	0.098	7.89	0.098	7.89	8.77
	C_2H_6	0.050	8.68	0.050	8.62	9.47
Wabasca [29]	N_2	0.230	16.03	0.000	16.93	19.91
	CO_2	0.094	6.91	0.084	6.90	8.88
	C_2H_6	0.028	6.65	0.028	6.55	6.56
JACOS [31]	C_2H_6	0.010	9.83	0.010	9.84	
Surmont [30,31]	C_2H_6	0.000	6.94	0.000	7.31	
	C_3H_8	0.066	6.83	0.063	6.52	
	C_4H_{10}	0.076	8.74	0.076	7.77	

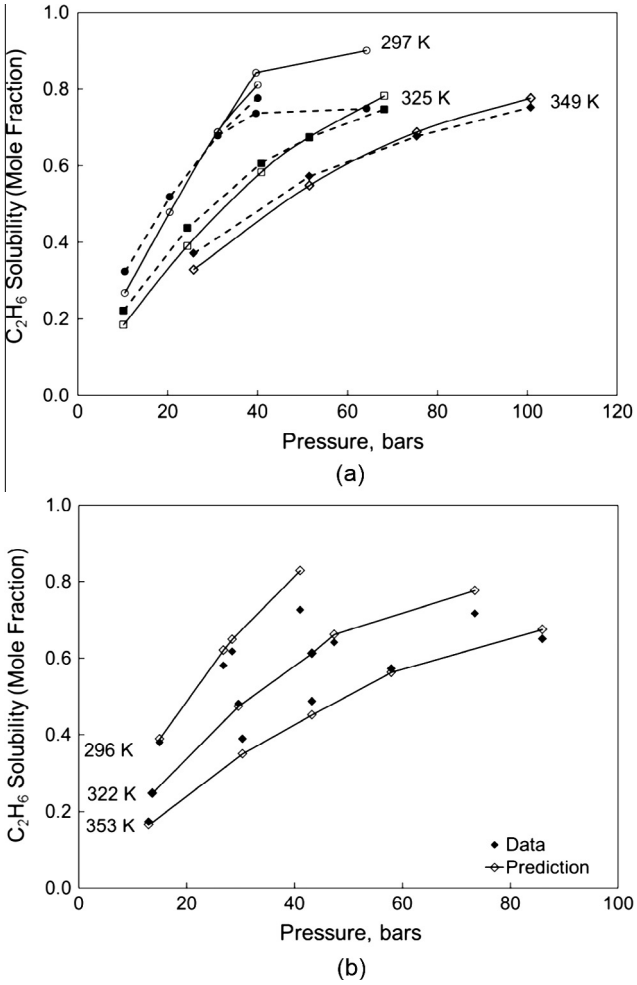

Fig. 2. Comparison of the data and predictions for ethane solubilities for (a) Cold Lake and (b) Athabasca bitumens. For Cold Lake bitumen, solid curves show the predictions and dashed curves show the data.

paper. Fig. 2 compares the ethane solubilities calculated based on the PnA method and the corresponding data for Cold Lake (Fig. 2a) and Athabasca (Fig. 2b). This figure indicates that the bitumen model has been better calibrated at higher temperatures likely because the methane saturation pressure, P_S, used was taken from near 373 K.

The AARD for CO_2 solubilities at 91 pressure–temperature points for all bitumens is 6.05% in the 4-PC case and 6.06% in the 1-PC case. For Athabasca, the AARD is 5.6% with PnA method (the 1-PC and 4-PC cases), 7.3% with the characterization by Mehrotra and Svrcek [10] with five pseudo components, and 9.34% by Kariznovi et al. [12] with six pseudo components. For Wabasca, the AARD is 6.9% with the PnA method (the 1-PC and 4-PC cases), 4.1% by Mehrotra and Svrcek [11], and 8.88% by Kariznovi et al. [12]. Experimental data for the Cold Lake bitumen shows that the CO_2 solubility levels off at an increased pressure along some isotherms, and that some solubility isotherms cross each other. Fig. 3 compares the CO_2 solubilities calculated based on the PnA method with the corresponding data for the Cold Lake bitumen. The above-mentioned characteristics are observed for the data and predictions for 288 K and 299 K.

The gas-solubility data for the JACOS and Surmont bitumens contain the liquid–liquid (L–L) equilibrium in addition to the liquid–vapor (L–V) equilibrium. It was observed in this research that a positive BIP was required to match L–L data using the PnA method, but the use of a positive BIP did not affect the L–V predictions significantly. For example, the optimized BIP between propane and the single bitumen component is 0.066 for the Surmont bitumen as given in Table 2. The L–L data could not be matched with zero BIP for propane and the bitumen component.

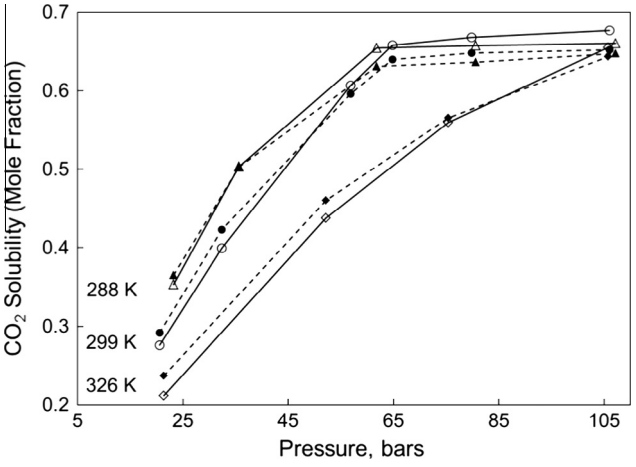

Fig. 3. Comparison of calculated CO_2 solubilities and data for Cold Lake bitumen. The solid lines shows the calculated values, and the dashed lines shows the data. Solubilities at 288 and 299 K are nearly constant at pressures above 65 bars. It is also observed that the solubility at 288 K is lower than that at 299 K for pressure above 65 bars.

It is important to analyze the sensitivity of bitumen characterization to the MW used in Step 1 of bitumen characterization, considering the inherent uncertainty in the quality of bitumen samples. The JACOS bitumen is re-characterized using the 1-PC PnA method assuming different MWs by perturbation of the MW between −15% and +15%. Then, predictions are made for methane solubilities and ethane solubilities. The BIP for methane with the bitumen is zero, and that for ethane with the bitumen is 0.01. Fig. 4 shows the variation of AARDs with respect to MW deviation. The variation in AARD is quite small; e.g., it is less than 2.25% between −15% and +15% deviations in MW for the ethane solubility. A higher AARD for the ethane solubility may be because of the same BIP of 0.01 was used for all cases for the MW variation. The results indicate that the PnA method of bitumen characterization is not much affected by the uncertainty of bitumen MW. However, it is important to use reliable data for the density at a saturation pressure for a gas-saturated bitumen because it directly affects the a and b parameters in the PnA method.

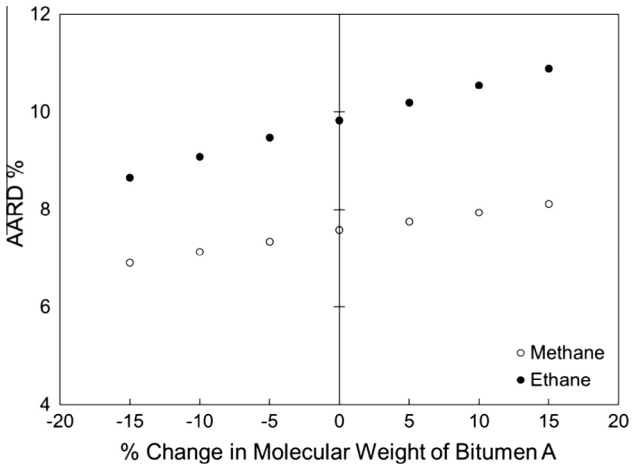

Fig. 4. AARDs for methane and ethane solubilities in the JACOS bitumen with different MWs used in the PnA algorithm.

2.3. Reliable trends for ψ and b with respect to MW

Kumar and Okuno [17] established qualitative trends for ψ and b with respect to CN (or MW) and aromaticity by use of the PR EOS. The PnA method, as implemented in this paper for bitumen characterization, is designed to keep reasonable trends for ψ and b when matching a saturation pressure and liquid densities. This is a highly implicit process with the conventional methods that change many parameters (e.g., T_C, P_C, and ω for pseudo components) individually to match various types of available data.

In this subsection, trends of these parameters are shown for Athabasca bitumen characterized by the PnA method. They are compared with those calculated by using the sets of T_C, P_C, and ω presented by Kariznovi et al. [12] and Mehrotra et al. [10] for the same Athabasca bitumen (Fig. 5a and b). It can be observed that the qualitative trends of ψ and b for the PnA method and Kariznovi et al. [12] are similar to each other. However, the trends for Mehrotra and Svrcek [10] are significantly different. Matching a limited amount of data by the PR EOS is possible with unreasonable trends, but the resulting model may not give reliable predictions at thermodynamic conditions away from the experimental conditions, according to the research by Kumar and Okuno [17].

With the PnA method, it is easy to preserve reliable trends for ψ and b during the regression to experimental data for two reasons: (1) the two parameters (ψ and b) for all pseudo components are systematically adjusted through only two adjustment parameters (f_b and f_ψ) from the n-alkane values that have been optimized for the PR EOS to give accurate phase behavior predictions, and (2) liquid densities are properly used to capture the effect of aromaticity on the a (or ψ) and b parameters. It is not easy for conventional methods to achieve reliable trends for ψ and b, especially when a limited amount of experimental data are available. With only one data point of saturation pressure for a particular gas with bitumen, for example, the conventional methods will attempt to match it by adjusting T_C, P_C, and ω of all pseudo components (say, 6 pseudo components), which is subject to a high level of non-uniqueness and may result in absurd trends of a (or ψ) and b. In conventional methods, density data are not effectively used for determination of T_C, P_C, and ω of pseudo components since they are matched by volume shift. Use of liquid density data in the PnA method is particularly important because ψ (or a) and b can be reliably adjusted to match a saturation pressure and density, respectively. This novel feature of the PnA method enables to characterize bitumen as a single component without substantially affecting gas solubility predictions, unlike conventional bitumen-characterization methods.

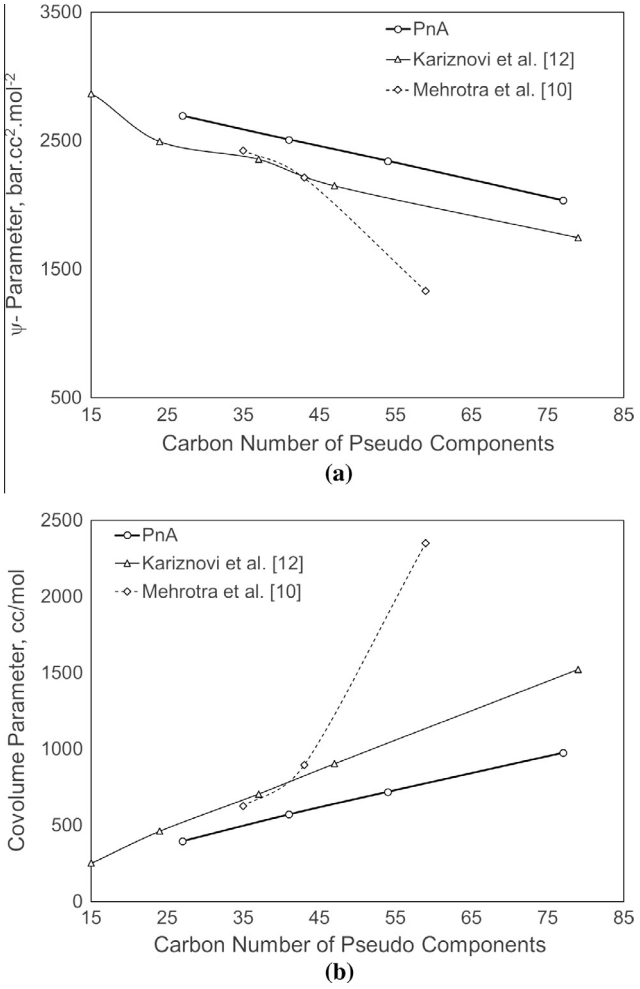

Fig. 5. Comparison of the ψ and b parameters from different characterizations for Athabasca bitumen: (a) the ψ parameter, (b) the covolume parameter.

3. Sensitivity analysis for oleic-phase viscosity at chamber edge

Results in the previous section indicate that, with the PnA method developed, the usage of one pseudo component (the 1-PC case) yields a similar level of accuracy to that of four pseudo components (the 4-PC case) in terms of gas solubility calculations. However, they may still exhibit substantial differences when used in flow simulation of steam-solvent coinjection for bitumen recovery. This is because bitumen recovery in such processes is dependent mainly on the L-phase viscosity near the steam-chamber edge. Currently, however, the effect of bitumen characterization (e.g., the number of pseudo components used) on bitumen recovery simulation can be evaluated only by running multiple flow simulations with different sets of fluid models, which is time-consuming. This section presents a new analytical method to evaluate the sensitivity of coinjection simulation results to bitumen characterization, without running actual flow simulations.

The main idea is to see if there is a substantial difference between the lightest and heaviest pseudo components of a multi-component model in terms of viscosity when they are treated as a single-component bitumen and mixed with solvent at the chamber-edge conditions. If the difference is small, the pseudo components (bracketed by the lightest and heaviest) likely behave similarly in thermal flow simulation, and may be modeled as a grouped single component. Otherwise, use of multiple components is recommended for proper representation of bitumen for steam-solvent coinjection simulation.

3.1. Estimation of temperature, oil-phase composition, and viscosity at chamber edge

The first step is to estimate the temperature and oil-phase composition at a steam-chamber edge, which significantly affect oil recovery in coinjection. A chamber edge is defined where the phase transition occurs between the oil–water (L–W) and vapor–oil–water (V–L–W) phase equilibria; hence, it is where the V phase (dis)appears. A brief description of the L-phase composition at a chamber edge is given below.

The thermodynamic formulation is based on the following assumptions as conventionally done in this area of research: (a) ternary mixtures of water, a solvent component, and a bitumen component; (b) complete immiscibility between the W and L phases; (c) Raoult's law for partitioning of the water component between the W and V phases; and (d) hydrocarbon K values based on the PR EOS. The water, oil, and solvent components are labeled

with indices i = w, o, and s, respectively. The W, L, and V phases are expressed using indices j = W, L, and V, respectively. x_{ij} is the mole fraction of component i in phase j. Then, phase equilibrium for such a ternary three-phase system at a given temperature (T) and pressure (P) is

$$P_w^{vap} = x_{wV}P \tag{5}$$

$$x_{oV} = K_o x_{oL} \tag{6}$$

$$x_{sV} = K_s x_{sL} \tag{7}$$

$$x_{oL} + x_{sL} = 1.0 \tag{8}$$

$$x_{wV} + x_{oV} + x_{sV} = 1.0, \tag{9}$$

where P_w^{vap} is the vapor pressure of water at T, and K_i is the K value for component i. Eq. (5) is for the V–W equilibrium, and Eqs. (6) and (7) are for the V–L equilibrium. Eqs. (8) and (9) are summation constraints. Note that the W phase consists of only water, and the L phase contains no water, due to assumption (*b*).

Using the multiphase Rachford–Rice procedure [32], it is easy to solve for the L-phase composition (χ_{iL}; i = {o, s}) at a given P and T because the compositions of three equilibrium phases are uniquely determined for a ternary system at a given P and T. The L-phase composition so obtained corresponds to the one at the chamber-edge temperature (T_e) at a given P; that is, the specified T is taken as T_e. This procedure gives the relationship between the L-phase composition and temperature at the chamber edge for a given operating pressure for a specified solvent-bitumen system. More details of similar calculations for T_e and L-phase composition can be found in Keshavarz et al. [8].

Once the relationship between T_e and the L-phase composition at P is set, the second step is to calculate the L-phase viscosity through a certain model. The following viscosity model has been implemented in the STARS reservoir simulator [33]:

$$\ln \mu_{mix} = \sum_{i=1}^{N_C} x_i \ln \mu_i, \tag{10}$$

which is used in this section in order to keep the consistency with the simulation case study given in Section 4. In Eq. (10), x_i and μ_i are the mole fraction and the effective viscosity of component i, respectively. N_C is the number of components in the phase for which the viscosity, μ_{mix}, is calculated (N_C = 2 in this section because only the o and s components are present in the L phase). Note that an effective viscosity is in general different from the viscosity of that component because it is determined by matching experimental viscosity data for mixtures using Eq. (10).

Experimental data are used for μ_o for the 1-PC bitumen. For the 4-PC case, μ_o for each pseudo component is determined by fitting Eq. (10) to that of the 1-PC bitumen using the known overall composition. An effective viscosity for a gas or solvent (e.g., methane and solvent components used in steam-solvent coinjection) is determined by fitting Eq. (10) to experimental viscosity data for a given composition. When experimental data are not available for the bitumen/gas system of interest, correlations (e.g., the corresponding state viscosity model [34]) can be used to obtain a reasonable estimation of an effective viscosity for the gas/solvent, as in the next subsection.

In the third, last step, two curves for μ_{mix} at T_e for an operating P with a specific solvent coinjected with steam are plotted along the mixing line between 100% solvent and 100% bitumen; one with the lightest pseudo component, and the other with the heaviest pseudo component, in a multi-component representation of bitumen. Note that T_e varies with the L-phase composition, through the temperature dependency of K values. That is, the resulting μ_{mix} function has taken into account the effect the varying temperature on μ_{mix}. If a large difference is observed for the two curves along the mixing line between the solvent and bitumen, use of multiple pseudo components is recommended for proper representation of bitumen in the steam-solvent coinjection of interest. Otherwise, a single-component bitumen model is likely sufficient. For further explanation, an example calculation will be shown using the JACOS bitumen in the next subsection.

3.2. Application to JACOS Bitumen

The analytical method given in Section 3.1 is applied to JACOS bitumen. The sensitivity of the L-phase viscosity at T_e at a typical operating pressure (35 bars) to the number of pseudo components used in bitumen characterization is studied for different single-component solvents, n-alkanes from C_3 to C_{10}. The 4-PC and 1-PC representations are compared.

The JACOS bitumen was characterized in Section 2. However, it is re-characterized here using unequal mass fractions, in place of the equal mass used previously. This is to have a wider variety of pseudo components in terms of volatility, which is expected to amplify the difference in terms of μ_{mix} among pseudo components in the analytical method. Table 3 presents the resulting 4-PC model along with the original 4-PC and 1-PC models from Section 2. The mass fraction is 0.85 for the heaviest and 0.05 for the lightest pseudo component.

Fig. 6 compares the temperature–composition (T–x) diagrams for binary mixtures of C_3 with different pseudo components. Fig. 6a uses 4 pseudo components on the equal mass basis (from Section 2) and the 1-PC model. Fig. 6b uses 4 pseudo components on the unequal mass basis and the 1-PC model. As expected, the latter shows a larger difference between the lightest (4-PC-L) and heaviest (4-PC-H) pseudo components in terms of two-phase envelope with C_3.

BIPs of solvents with pseudo components are based on the correlation developed using experimental data as follows:

$$k_{sb} = 0.0349 \ln\left(\frac{V_{c,s}}{V_{c,b}}\right) + 0.1329 \tag{11}$$

where k_{sb} is the BIP between the solvent and bitumen components. $V_{c,s}$ and $V_{c,b}$ are the critical volumes of the solvent and bitumen components, respectively. They can be obtained from Step 5 of the PnA algorithm (see Section 2.1). As evident from Table 1, the JACOS and Surmont bitumens are similar to each other in terms of MW, methane solubilities, and characterization parameters (f_b and f_ψ). Hence, Eq. (11) was developed by using optimized BIPs for propane and butane solubilities in the Surmont bitumen sample.

Table 3
Molecular weights, T_C, P_C, and ω for pseudo components of JACOS bitumen [30].

Pseudo component		MW	T_C (K)	P_C (bars)	ω
Bitumen as single pseudo component					
1-PC		530.00	847.17	10.64	1.0406
Pseudo components	**Mole fraction**	**MW**	**T_C (K)**	**P_C (bars)**	**ω**
Bitumen split into four pseudo components with equal mass fractions					
4-PC-1	0.4001	331.77	775.08	14.36	0.81599
4-PC-2	0.2616	507.44	859.24	11.05	1.03422
4-PC-3	0.1995	665.41	905.82	9.27	1.16443
4-PC-4	0.1388	956.63	946.51	7.16	1.32306
Bitumen split into four pseudo components with different mass fractions					
4-PC-1	0.1189	222.88	686.53	18.07	0.59623
4-PC-2	0.0868	305.20	751.60	15.01	0.76675
4-PC-3	0.0751	353.73	781.52	13.73	0.84498
4-PC-4	0.7192	626.41	887.27	9.58	1.13115

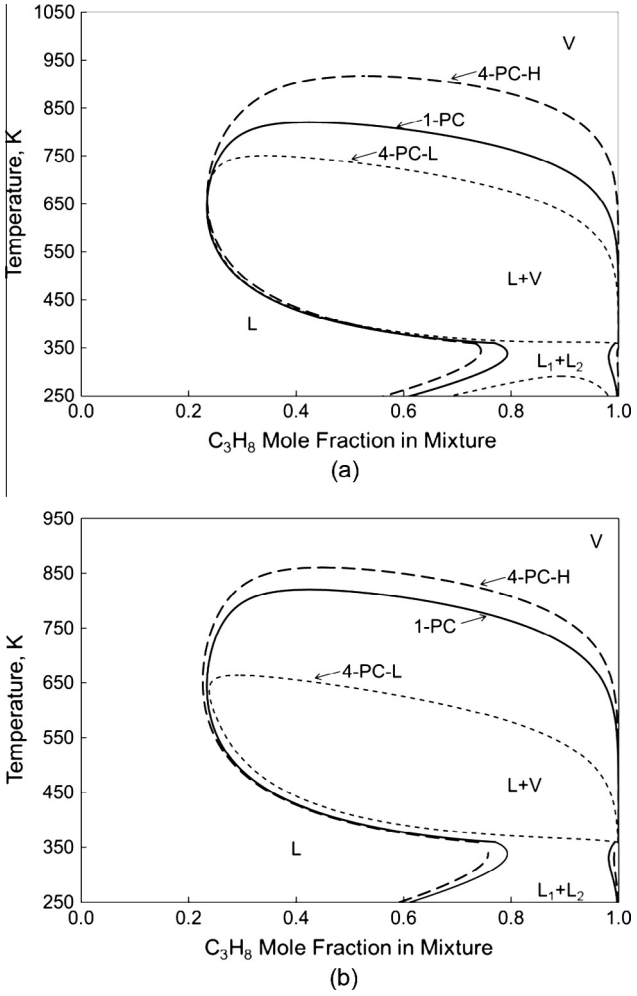

Fig. 6. Comparison of T–x diagrams at 35.0 bars for bitumen–propane mixtures for two different compositional characterizations of the JACOS bitumen; (a) the same mass fraction (0.25) for all pseudo components, and (b) different mass fractions (0.05 for 4-PC-L and 0.85 for 4-PC-H). The envelope shown by solid curve is for the 1-PC model, and the dashed curves are for 4-PC-L and 4-PC-H.

Then, K values are obtained for water and hydrocarbon components at 35 bars, as described in the previous section. Raoult's law is used for partitioning of water between the V and W phases. The PR EOS model is used for L–V equilibrium for binary systems, each of which consists of a solvent component and a pseudo component (the lightest or the heaviest pseudo component). The K values are then used to obtain the relationship between T_e and the L-phase composition as explained in Section 3.1 (the first step). Since the L phase does not contain the water component, T_e is given as a function of x_{sL} for each of the lightest and heaviest pseudo components.

Viscosity data is available for mixtures of the JACOS bitumen with methane, but not with other gases. Therefore, viscosity data for the Surmont bitumen and solvent gases [31] were also used to develop the viscosity model. On the basis of experimental data, the effective viscosities for methane and propane have been obtained at 35 bars at different temperatures. Effective viscosities for other solvent components are estimated by using a corresponding state method, which is similar to [34]. Fig. 7 shows the effective viscosities with varying temperature at 35 bars obtained for different solvents. The number next to each curve is the solvent CN.

Finally, Eq. (10) is used with the effective viscosities and the relationship between T_e and x_{sL} at 35 bars for the lightest and heaviest pseudo components for each solvent. This gives the L-phase viscosity at the chamber-edge conditions (μ_{edge}) as a function of

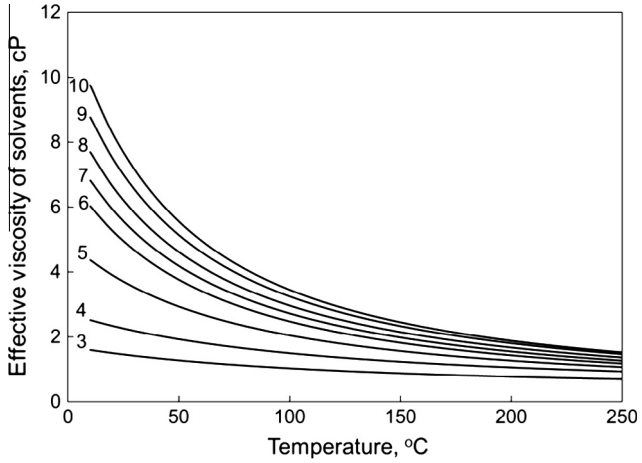

Fig. 7. Effective viscosities of solvents at 35.0 bars. The number next to each curve is the solvent carbon number.

x_{sL} for each solvent/pseudo-component pair. Fig. 8a, b, and c respectively present the results for C_3, C_4, and C_6. In each figure, μ_{edge} for the 1-PC model is also given as a reference. The difference between the μ_{edge} curves for the lightest and heaviest pseudo components is the largest for the C_3 coinjection case, and diminishes as the solvent becomes heavier. In Fig. 8a–c, μ_{edge} at the lower and higher ends of x_{sL} are determined by the viscosities of bitumen components (i.e., 1-PC, 4-PC-L, 4-PC-H) and solvents. It is important to analyze the trends in the mid-range of x_{sL}.

The μ_{edge} trends in the mid-range of x_{sL} are affected by two main factors: (1) T_e and (2) the sensitivity of bitumen viscosity to temperature. For a given bitumen component, T_e increases with increasing CN of solvent, or decreasing volatility of solvent. The sensitivity of bitumen viscosity to temperature is more significant at lower temperatures than at higher temperatures; e.g., viscosity data for JACOS bitumen show −115 cp/K at 345 K and −0.45 cp/K at 445 K at 35 bars.

Let us consider two μ_{edge} values at x_{sL} of 0.5 at 35 bars: one for propane with 4-PC-L and the other for propane with 4-PC-H. The T_e is 401 K for the 4-PC-L and 390 K for the 4-PC-H component. The propane viscosity at these conditions is calculated to be nearly constant, around 0.95 cp. However, the viscosity of the 4-PC-L component is 61.0 cp at 401 K, and that of the 4-PC-H component is 100.6 cp at 390 K. The difference in viscosity between the two bitumen components yields the difference observed in Fig. 8a.

The same analysis is made for the butane case (Fig. 8b). The T_e is 451 K for the 4-PC-L and 438 K for the 4-PC-H. The butane viscosity at these conditions is calculated to be approximately 1.1 cp. However, the viscosity of the 4-PC-L component is 15.14 cp at 451 K, and that of the 4-PC-H component is 21.13 cp at 438 K.

As the solvent becomes less volatile, T_e increases and the impact of varying bitumen viscosity becomes less significant on the calculated μ_{edge}. Hence, the highest contrast in the trends of μ_{edge} with respect to x_{sL} for 4-PC-L and 4-PC-H is observed in the case of propane, the lightest solvent tested in this research.

4. Simulation case study

This section shows the simulation case study for steam-solvent coinjection for the JACOS bitumen based on the reservoir model used in Keshavarz et al. [5]. The simulation is performed using the STARS simulator [33] with the phase behavior models from the 4-PC and 1-PC cases (see Table 3). Results from Section 3 indicate that the simulation of C_3-steam coinjection for the JACOS bitumen may be sensitive to the number of pseudo components used for bitumen characterization; that is, use of the 4-PC model may

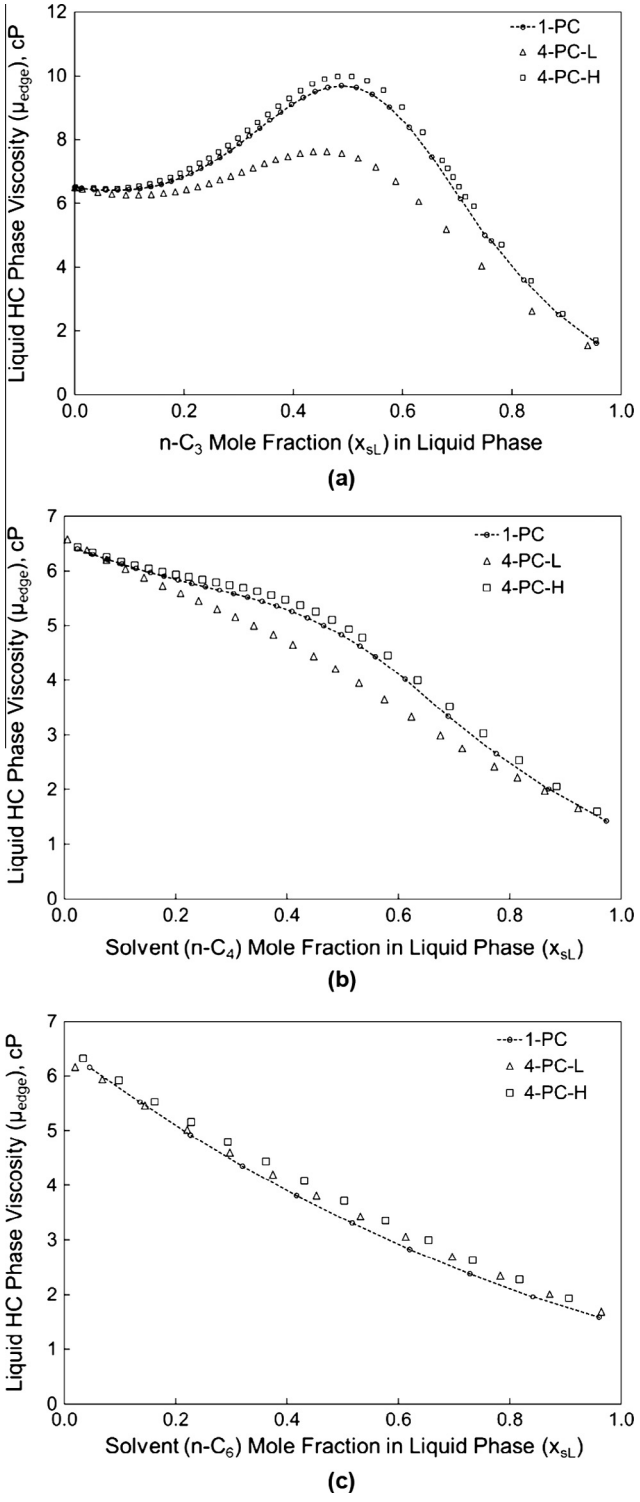

Fig. 8. Estimated trends for the L-phase viscosity at the chamber-edge conditions (μ_{edge}) with respect to the solvent mole fraction in the L-phase (x_{sL}); (a) propane-steam coinjection, (b) butane-steam coinjection, and (c) hexane-steam coinjection.

result in different simulation results than that of the 1-PC model. This will be validated in this section.

The reservoir and fluid properties are summarized in Table 4. This is a vertical-cross-sectional 2-D reservoir with 70 (horizontal) × 20 (vertical) grid blocks. The uniform grid-block size is 1.0 × 37.5 × 1.0 m. Grids are numbered from left to right in the horizontal direction, and from top to bottom in the vertical direction. The injector is located at the grid bock (1, 14), and the producer is at (1, 18); i.e., only a half of a steam chamber is simulated.

Table 4
Reservoir and fluid properties used in recovery simulation of JACOS bitumen.

Properties	Values
Porosity	33%
Horizontal permeability	4000 md
Vertical permeability	3000 md
Initial reservoir pressure at depth of 500 m	1500 kPa
Initial reservoir temperature	13 °C
Initial oil saturation	0.75
Initial water saturation	0.25
Three-phase relative permeability model [33]	Stone's model II
Formation compressibility	1.8E−5 1/kPa
Rock heat capacity [1]	2600 kJ/m^3 °C
Rock thermal conductivity [1]	660 kJ/m day °C
Over/underburden heat capacity [1]	2600 kJ/m^3 °C
Over/underburden thermal conductivity [1]	660 kJ/m day °C
Bitumen thermal conductivity [1]	11.5 kJ/m day °C
Gas thermal conductivity [35]	2.89 kJ/m day °C
Water thermal conductivity	1500 kJ/m day °C
Bitumen molecular weight	530 kg/kg mol
Bitumen specific gravity	1.077
Injector bottom-hole pressure (maximum)	3500 kPa
Producer bottom-hole pressure (minimum)	1500 kPa
Producer steam flow rate (maximum)	1 m^3/day
Steam quality	0.9
Temperature of injected steam	242.71 °C

The gas-to-oil ratio is assumed to be 4 Sm^3/Sm^3, for which the reservoir oil consists of 91 mol% bitumen and 9 mol% methane. The solvents tested are n-alkanes between C_3 and C_{10}. The coinjection pressure is 35 bars, at which the saturation temperature of water is 515.86 K. The *K* values for water, solvents, and pseudo component(s) of bitumen are generated using the Winprop software [33] for 80 mol% reservoir-oil and 20 mol% solvent. The injectant consists of 2 mol% single-component solvent and 98 mol% water.

The viscosity model used was given in Section 3. The density data are available for mixtures of bitumen with methane and propane. Densities for mixtures of bitumen and other solvents can be calculated by using the EOS models (Table 3). However, the STARS simulator uses

$$\frac{1}{\rho_L} = \sum_{i=1}^{N_C} \frac{\chi_{iL}}{\rho_{iL}} \tag{12}$$

to calculate the L-phase density. Therefore, the L-phase density values from experimental data and EOS models are used to calculate the effective densities of components in the L phase using Eq. (12). In this equation, ρ_L is the molar density of the L phase, χ_{iL} is the mole fraction of component *i* in the L phase, and ρ_{iL} is the effective molar density of component *i* in the L phase. The starting value for ρ_{iL} is obtained from the *a* and *b* parameters for component *i* with the PR EOS at the pressure and temperature. Then, ρ_{iL} are regressed to match ρ_L with Eq. (12). Other parameters, such as liquid compressibility, coefficients of thermal expansion, enthalpy, are generated using the Winprop software [33] with the EOS models.

Production starts after six months of preheating for achieving the thermal communication between the injector and the producer. Fig. 9 presents the bitumen production histories for four cases of coinjection: C_3, C_4, C_5, and C_6. For each solvent coinjection case, two curves are given for the 4-PC and 1-PC bitumen models. The recovery histories for heavier solvent cases are nearly identical with the C_6 coinjection case, and not shown in Fig. 9. In general, bitumen production is more rapid in coinjection of heavier solvent because of higher T_e and dilution of bitumen. Although an optimum solvent should be selected based on economic evaluations of the entire process, Fig. 9 indicates the effect of solvent on bitumen production may diminish at CN 5 in these simple simulations.

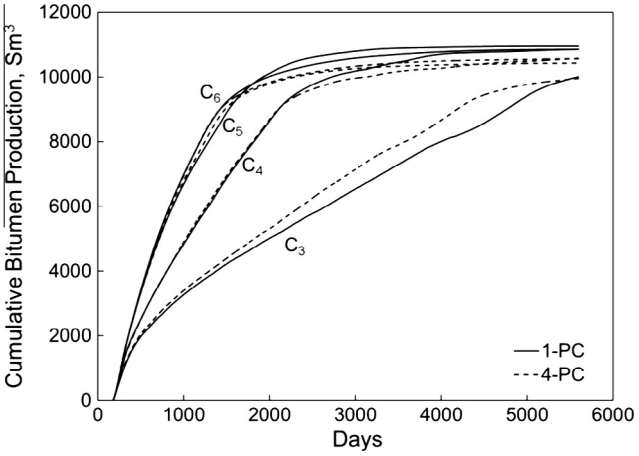

Fig. 9. Simulated bitumen recovery for ES-SAGD with different solvents, C_3, C_4, C_5, and C_6.

Fig. 9 shows that the difference between the 4-PC and 1-PC cases is pronounced for the C_3-steam coinjection case. This is because different pseudo components behave differently in the coinjection simulation in terms of the L-phase viscosity, which is the primary factor affecting bitumen production. The difference in phase behavior can be quantified by looking at the difference between the lightest and heaviest pseudo components (4-PC-L and 4-PC-H). The results given in Fig. 9 is in line with the observation from the previous section that the μ_{edge} curves for the 4-PC-L and 4-PC-H exhibit more deviation for the C_3 coinjection case than for coinjection of heavier solvents. This simulation case validates the simple procedure developed for assessing the sensitivity of coinjection simulation to the number of bitumen components.

Fig. 10 shows μ_{edge} simulated along the chamber edge in the C_3, C_4, and C_6 coinjection cases using the 4-PC and 1-PC models after 580 days of production. The horizontal axis in the figure is the number of grid block from the reservoir top. Note that the plots for the 4-PC cases come from the mixing of all components, including the coinjected solvent and 4 pseudo components. The simulated μ_{edge} shows the largest difference between the 4-PC and 1-PC cases for the C_3 coinjection case. The difference diminishes as the coinjected solvent becomes heavier. The absolute average deviation (AAD) for μ_{edge} between the 4-PC and 1-PC cases is 1.64 cp for C_3 coinjection, 0.31 cp for C_4 coinjection, and 0.21 cp for C_6 coinjection.

5. Conclusions

A new analytical method was presented for assessing the sensitivity of ES-SAGD simulation to the number of components used for bitumen characterization. The method was compared with the flow simulation based on experimental phase-behavior data and reliable bitumen characterization. The PnA method of fluid characterization was modified and applied for the first time to bitumen characterization. Conclusions are as follows:

- The analytical method for assessing the effect of bitumen characterization on ES-SAGD simulation results was successfully validated in the simulation case study. Use of multiple pseudo components is recommended if the lightest and heaviest pseudo components from a multi-component representation of bitumen behave differently in terms of the L-phase viscosity at chamber-edge conditions. The analytical method can detect the sensitivity of ES-SAGD simulation to bitumen characterization without performing multiple flow simulations using different sets of fluid models.

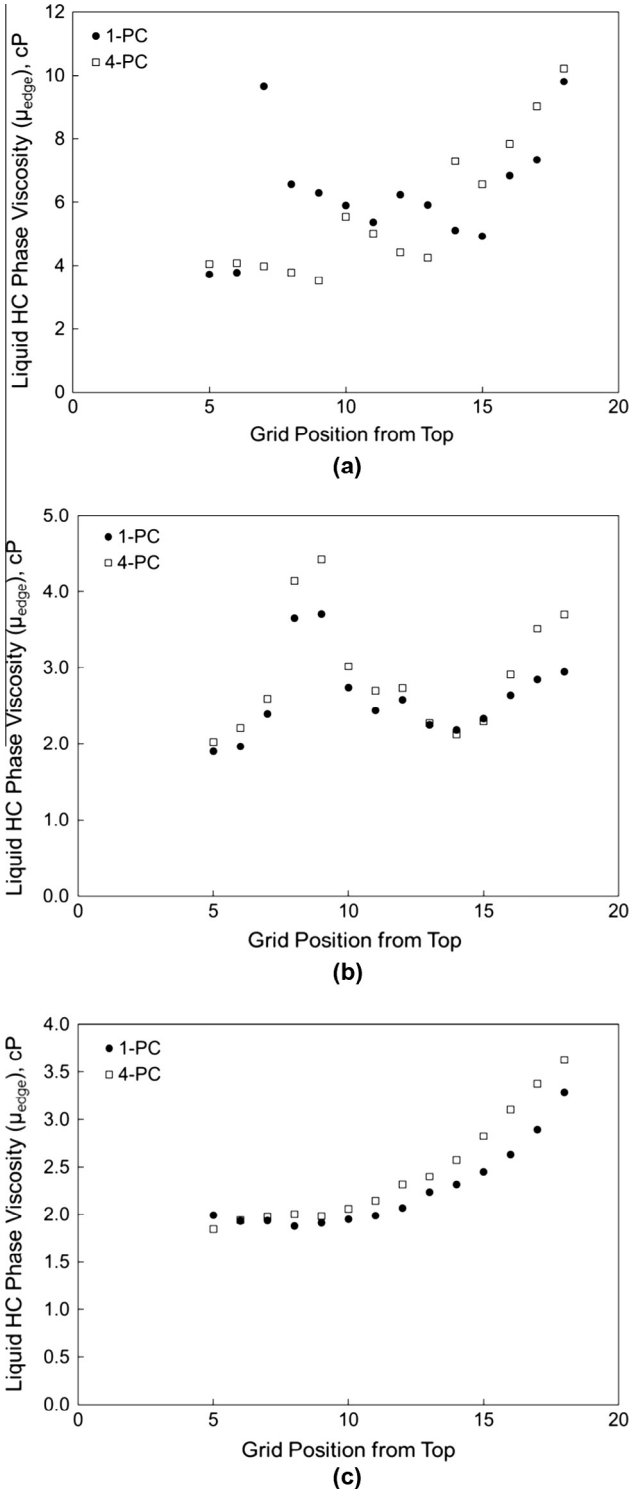

Fig. 10. L-phase viscosity along the chamber edge from the simulation results: (a) propane-steam coinjection, (b) butane-steam coinjection, and (c) hexane-steam coinjection. The number on the horizontal axis shows the grid's number from the reservoir top.

- The PnA method was modified and successfully applied to characterization of six different bitumens. With the PnA method, no obvious difference was observed between the one-component and four-component representations of bitumen in terms of the correlative accuracy for gas solubilities and densities using the PR EOS.

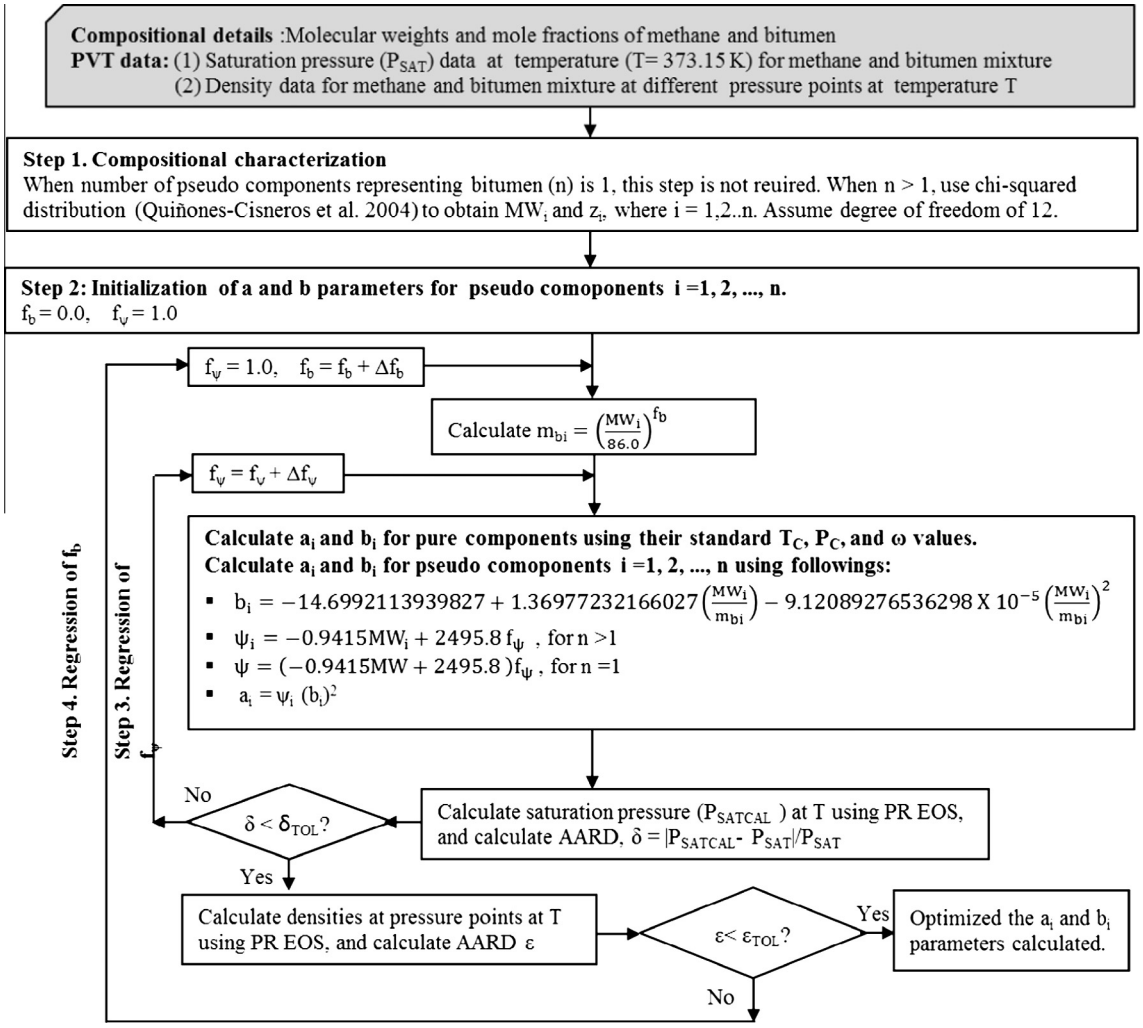

Fig. A1. Flow chart for the algorithm developed for bitumen characterization based on direct perturbation from n-alkanes.

- A proper number of pseudo components for bitumen characterization for ES-SAGD simulation cannot be determined without considering the effect of phase behavior on the L-phase viscosity at chamber-edge conditions. Results show that the one-component representation of bitumen may be sufficient for correlating gas solubilities and densities, but may not for reliable ES-SAGD simulation. This is because ES-SAGD simulation is substantially affected by the L-phase viscosity near the chamber edge, in which the gravity drainage of oil takes place.
- Matching L–L equilibrium data required positive BIPs between solvent and bitumen. The L–V equilibrium for bitumen and solvent was not sensitive to the BIPs used. Therefore, use of positive BIPs improved the accuracy of L–L representation without significantly affecting the accuracy of L–V representation.
- Bitumen characterization with the PnA method was not much affected by the uncertainty of bitumen MW. However, it is important for the PnA method to use accurate phase behavior data for saturation pressure and densities for gas-saturated bitumen.

Acknowledgments

This research was funded by the Natural Sciences and Engineering Research Council of Canada (RGPIN 418266), Japan Petroleum Exploration Co., Ltd., and Japan Canada Oil Sands Ltd.

Appendix A

See Fig. A1.

References

[1] Butler RM. Thermal recovery of oil and bitumen. Calgary, Alberta: Black book series, GravDrain Inc; 1997.
[2] Lake LW, Johns R, Rossen B, Pope G. Fundamentals of enhanced oil recovery. Richardson, Texas, USA: Society of Petroleum Engineers; 2014.
[3] Nasr TN, Beaulieu G, Golbeck H, et al. Novel expanding solvent-SAGD process "ES-SAGD". J Can Pet Technol 2003;42(1):13–6.
[4] Gupta S, Gittins SD. Christina lake solvent aided process pilot. J Can Pet Technol 2006;45(9):15–8.
[5] Keshavarz M, Okuno R, Babadagli T. Optimal application conditions for steam/solvent coinjection. SPE Res Eng Eval 2014;18(1):20–8.
[6] Nasr TN, Ayodele OR. New hybrid steam-solvent processes for the recovery of heavy oil and bitumen. In: Presented at Abu Dhabi international petroleum exhibition and conference, Abu Dhabi, U.A.E., 5–8 Nov. SPE-101717-MS; 2006.
[7] Jha RK, Kumar M, Benson I, et al. New insights into steam/solvent-coinjection-process mechanism. SPE J 2013;18(5):867–77.
[8] Keshavarz M, Okuno R, Babadagli T. A semi-analytical solution to optimize single-component solvent coinjection with steam during SAGD. Fuel 2015;144:400–14.
[9] James NE, Mehrotra AK. V-L-S multiphase equilibrium in bitumen-diluent systems. Can J Chem Eng 1988;66(5):870–8.
[10] Mehrotra AK, Svrcek WY. Characterization of Athabasca bitumen for gas solubility calculations. J Can Pet Technol 1988;27(6):107–10.
[11] Mehrotra AK, Patience GS, Svrcek WY. Calculation of gas solubility in Wabasca bitumen. J Can Pet Technol 1989;28(3):81–3.

[12] Kariznovi M, Nourozieh H, Abedi J. Bitumen characterization and pseudo components determination for equation of state modeling. Energy Fuels 2010;24(1):624–33.
[13] Whitson CH. Characterizing hydrocarbon plus fractions. SPE J 1983;23 (4):683–94.
[14] Lolley CS, Richardson WC. Minimum pseudocomponent requirements for compositional thermal simulation of heavy oil. In: Presented at SPE/DOE improved oil recovery symposium, Tulsa, Oklahoma, 19–22 April; 1998.
[15] Fu C-T, Puttagunta VR, Vilcsak G. Vapour-liquid equilibrium properties for pseudo-binary mixtures of CO_2-Athabasca and N_2-Athabasca bitumen. AOSTRA J Res 1985;2(2):73–81.
[16] Lu BC-Y, Chung WK, Adachi Y, et al. Correlation and prediction of solubilities of gases in Athabasca bitumen. AOSTRA J Res 1986;2(3):139–46.
[17] Kumar A, Okuno R. Direct perturbation of the Peng–Robinson attraction and covolume parameters for reservoir fluid characterization. Chem Eng Sci 2015;127:293–309.
[18] Peng D-Y, Robinson DB. A new two-constant equation of state. Ind Eng Chem Fund 1976;15(1):59–64.
[19] Peng D-Y, Robinson DB. The characterization of the heptanes and heavier fractions for the GPA Peng–Robinson programs. GPA Res Rep 1978. RR-28.
[20] Kumar A, Okuno R. Critical parameters optimized for accurate phase behavior modeling for heavy n-alkanes up to C_{100} using the Peng–Robinson equation of state. Fluid Phase Equilib 2012;335:46–59.
[21] Quiñones-Cisneros SE, Zéberg-Mikkelsen CK, Baylaucq A, et al. Viscosity modeling and prediction of reservoir fluids: from natural gas to heavy oils. Int J Therm 2004;25(5):1353–66.
[22] Lee BI, Kesler MG. A generalized thermodynamic correlation based on three-parameter corresponding states. AIChE J 1975;21:510–27.
[23] Kesler MG, Lee BI. Improved prediction of enthalpy of fractions. Hydrocarb Process 1976;55:153–8.
[24] Riazi MR, Daubert TE. Molecular weight of heavy fractions from viscosity. Oil Gas J 1987;58(2):110–3.
[25] Svrcek WY, Mehrotra AK. Gas solubility, viscosity and density measurements for Athabasca bitumen. J Can Pet Technol 1982;21(4):31–8.
[26] Mehrotra AK, Svrcek WY. Viscosity, density and gas solubility data for oil sand bitumens. Part I: Athabasca bitumen saturated with CO and C_2H_6. AOSTRA J Res 1985;1(4):263–8.
[27] Mehrotra AK, Svrcek WY. Properties of Cold Lake bitumen saturated with pure gases and gas mixtures. Can J Chem Eng 1988;66(4):656–65.
[28] Mehrotra AK, Svrcek WY. Viscosity, density and gas solubility data for oil sand bitumens. Part II: Peace river bitumen saturated with N_2, CO, CH_4, CO_2 and C_2H_6.. AOSTRA J Res 1985;1(4):269–79.
[29] Mehrotra AK, Svrcek WY. Viscosity, density and gas solubility data for oil sand bitumens. Part III: Wabasca bitumen saturated with N_2, CO, CH_4, CO_2, and C_2H_6.. AOSTRA J Res 1985;2(4):83–93.
[30] Kariznovi M. Phase behaviour study and physical properties measurement for Athabasca bitumen/solvent systems applicable for thermal and hybrid solvent recovery processes [Ph.D. thesis]. University of Calgary, Alberta, Canada; 2013.
[31] Nourozieh H. Phase partitioning and thermo-physical properties of Athabasca bitumen/solvent mixtures [Ph.D. thesis]. University of Calgary, Alberta, Canada; 2013.
[32] Okuno R, Johns RT, Sepehrnoori K. A new algorithm for Rachford–Rice for multiphase compositional simulation. SPE J 2010;15(2):313–25.
[33] Computer Modelling Group (CMG) Ltd. Version 2012. Calgary, Alberta, Canada; 2012.
[34] Lindeloff N, Pedersen KS, Ronningsen HP, et al. The corresponding states viscosity model applied to heavy oil systems. J Can Pet Technol 2004;43 (9):47–53.
[35] Yazdani A, Alvestad J, Kjonsvik D, et al. A parametric simulation study for solvent co-injection process in bitumen deposits. In: Presented at the Canadian unconventional resources conference, Calgary, Alberta, Canada, 15–17 November. SPE-148804-MS; 2011.